

Missile Guidance Law Design via Backstepping Technique

Hamza Zaidi, Panlong Wu, Ali Bellahcene

Abstract — In this paper a Back-stepping Control technique is proposed for command to line-of-sight missile guidance law design. In this design, the three-dimensional (3-D) CLOS guidance problem is formulated as a tracking problem of a time-varying nonlinear system. Simulation results for different engagement scenarios illustrate the validity of the proposed Backstepping-based Guidance Law.

Index Terms—Command line-of-sight (CLOS), Backstepping Control system, missile guidance law.

I. INTRODUCTION

The Concept of command to line-of-sight (CLOS) guidance is to oblige (force) a missile to fly as nearly as possible along the instantaneous line-of-sight (LOS) between the land tracker and the target. If the missile can continuously stay on the LOS, missile will intercept the target. To set demanded accelerations for the missile, a guidance controller is used at the ground station to take computation of tracker information about the missile and target position, angular velocity and acceleration of the LOS. These acceleration commands can then be transmitted to the missile by a radio link. The CLOS guidance has been identify as a low-cost guidance concept because it conformance placement of avionics on the launch platform, as opposed to mounting on the expendable weapons [1], [2]. Theoretically, the missile-target model is nonlinear and time-varying. Many different guidance laws have been developed over the years, and with the advent of highly maneuverable targets, research on improved guidance laws is continuing [3]–[5].

In this study, a Backstepping control system is proposed for commanding line-of-sight CLOS. The Lyapunov stability theorem is used to ensure the stability of the control system. Simulations results demonstrate the effectiveness of the proposed control.

This paper is organized as follows. Formulation of missile-target engagement is described in Section II. The design procedures of the proposed Backstepping guidance system are constructed in Section III. Simulation results are set to confirm the effectiveness of the proposed control system in Section IV. Conclusions are drawn in Section V.

Hamza Zaidi, School of Automation, Nanjing University of Science and Technology, Nanjing, China, (+86) 13605146954.

Panlong Wu, School of Automation, Nanjing University of Science and Technology, Nanjing, China, (+86) 2584315172.

Ali Bellahcene, School of Automation, Nanjing University of Science and Technology, Nanjing, China, (+86) 15205191440.

Table I: Definition of symbols

Symbol	Description
ψ_t	Yaw angle of target
θ_t	Pitch angle of target.
ψ_m	Yaw angle of missile.
θ_m	Pitch angle of missile
ϕ_{mc}	Roll angle command.
σ_t	Azimuth angle of LOS to target.
γ_t	Elevation angle of LOS to target.
σ_m	Azimuth angle of LOS to missile
γ_m	Elevation angle of LOS to missile
$\Delta\sigma$	$\sigma_m - \sigma_t$
$\Delta\gamma$	$\gamma_m - \gamma_t$
g	Gravity acceleration.
a_x	Axial acceleration of missile
a_{yc}	Yaw acceleration command
a_{zc}	Pitch acceleration command.
a_{yt}	Yaw acceleration of target.
a_{zt}	Pitch acceleration of target.
R_m	Missile range from ground tracker.
R_t	Target range from ground tracker.

II. PROBLEMATIQUE OF THE THREE-DIMENSIONAL CLOS GUIDANCE

The three-dimensional CLOS guidance problem shown in Fig. 1 is a well-known guidance model [2], which involves guiding the missile along the LOS to the target. The three-dimensional CLOS guidance model in [5, 7] will be repeated here for convenience. The following description in Table 1 will be adopted to derive the dynamic equations of missile.

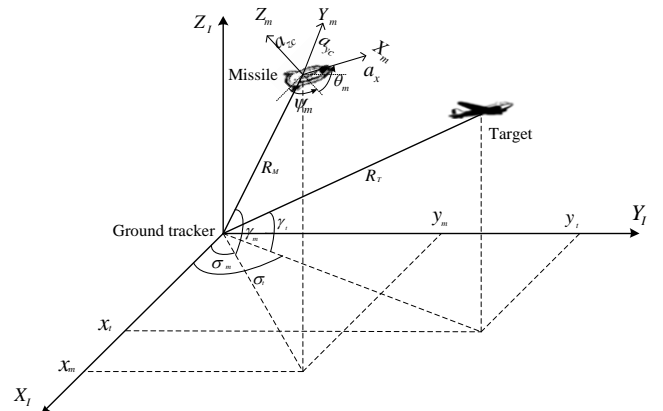


Fig. 1. Three-dimensional missile-target engagement diagram.

$$\begin{bmatrix} \ddot{x}_m \\ \ddot{y}_m \\ \ddot{z}_m \end{bmatrix} = \begin{bmatrix} c\theta_m c\psi_m & -s\phi_{mc}s\theta_m c\psi_m - c\phi_{mc}s\psi_m & -c\phi_{mc}s\theta_m c\psi_m + s\phi_{mc}s\psi_m \\ c\theta_m s\psi_m & -s\phi_{mc}s\theta_m s\psi_m + cs\phi_{mc}c\psi_m & -c\phi_{mc}s\theta_m s\psi_m - s\phi_{mc}c\psi_m \\ s\theta_m & s\phi_{mc}c\theta_m & c\phi_{mc}c\theta_m \end{bmatrix} \begin{bmatrix} a_x \\ a_{yc} \\ a_{zc} \end{bmatrix} - \begin{bmatrix} 0 \\ 0 \\ g \end{bmatrix}$$

$$\begin{bmatrix} \dot{\psi}_m \\ \dot{\theta}_m \end{bmatrix} = \begin{bmatrix} c\phi_{mc}/(v_m c\theta_m) & s\phi_{mc}/(v_m c\theta_m) \\ s\phi_{mc}/v_m & c\phi_{mc}/v_m \end{bmatrix} \begin{bmatrix} a_{yc} \\ a_{zc} \end{bmatrix} - \begin{bmatrix} 0 \\ gc\theta_m/v_m \end{bmatrix} \quad (1)$$

The origin of the inertial frame is located at the ground base. The axis Z_I is vertical upward and the $X_I - Y_I$ plane is horizontal. The origin of the missile body frame is fixed at the center of mass of missile, with the X_B axis forward along the missile centerline. The dynamics of the missile in the inertial frame can be represented [2] as described in (1) in the top of the page.

A tracking output is defined in order to convert the CLOS guidance problem into a tracking problem. The LOS frame is shown in Fig. 2 in which the origin of the three-dimensional space is located at the ground base. The X_L axis forwards along the LOS to the missile, and the Y_L axis is horizontal to the left of the X_L - Y_L plane. Then, the coordinates indicated in Fig. 2 represent the missile position in the LOS frame, and they are related to θ through rotations as follows:

$$\begin{bmatrix} z_1 \\ z_2 \end{bmatrix} = \begin{bmatrix} -s\sigma_t & c\sigma_t & 0 \\ -s\gamma_t c\sigma_t & -s\gamma_t s\sigma_t & c\gamma_t \end{bmatrix} \quad (2)$$

The tracking output is defined as $z \underline{\Delta}[z_1, z_2]^T$. Since z_1 and z_2 cannot be measured directly, these quantities must be computed indirectly using the polar position data of the missile available from the ground tracker as

$$z \underset{\Delta}{=} \begin{bmatrix} z_1 \\ z_2 \end{bmatrix} = \begin{bmatrix} R_m c(\Delta\gamma + \gamma_t) s\Delta\sigma \\ R_m (s(\Delta\gamma + \gamma_t) c\gamma_t - c(\Delta\gamma + \gamma_t) s\gamma_t) c\Delta\sigma \end{bmatrix} \quad (3)$$

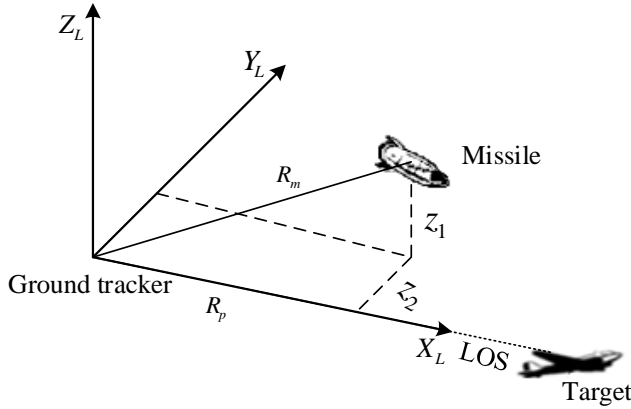


Fig. 2. Definition of tracking output.

Note that $\|z\|_2$ represents the distance from the missile to the LOS. Therefore, the missile will eventually intercept the target if the tracking output z_1 is driven to zero. The three-dimensional CLOS guidance problem therefore can be seen as a tracking problem. Define

$$\begin{aligned} x_{\underline{\underline{\Delta}}} &= [x_1 \quad x_2 \quad x_3 \quad x_4 \quad x_5 \quad x_6 \quad x_6 \quad x_7]^T \\ &\stackrel{\Delta}{=} [x_m \quad y_m \quad z_m \quad \dot{x}_m \quad \dot{y}_m \quad \dot{z}_m \quad \theta_m \quad \psi_m]^T \\ u_T \underline{\underline{\Delta}} &= [u_{T_1} \quad u_{T_2}]^T \stackrel{\Delta}{=} [a_{yc} \quad a_{zc}]^T \end{aligned} \quad (4)$$

Using the previous equations, (1), (2), and (4) can be put into the following dynamic equations of missile in state-space form:

$$\begin{aligned} \dot{x} &= f(x, t) + \sum_{j=1}^2 g_j(x) \cdot u_{T_j} \\ z &= h(x, t) \end{aligned} \quad (5)$$

where

$$f(x, t) = \begin{bmatrix} x_4 \\ x_5 \\ x_6 \\ a_x(t)cx_7cx_8 \\ a_x(t)cx_7cx_8 \\ a_x(t)cx_8 - g \\ 0 \\ -gcx_8 / (x_4^2 + x_5^2 + x_6^2) \end{bmatrix}$$

$$g_1(x) = \begin{bmatrix} 0 \\ 0 \\ 0 \\ -s\phi_{cm}sx_7cx_8 - c\phi_{cm}sx_7 \\ -s\phi_{cm}sx_7sx_8 + c\phi_{cm}cx_7 \\ s\phi_{cm} \cos x_8 \\ c\phi_{cm} / \left(x_4^2 + x_5^2 + x_6^2 \right)^{1/2} cx_8 \\ s\phi_{cm} / \left(x_4^2 + x_5^2 + x_6^2 \right)^{1/2} \end{bmatrix}$$

$$g_2(x) = \begin{bmatrix} -s\phi_{cm}/(x_4 + x_5 + x_6) \\ 0 \\ 0 \\ 0 \\ -c\phi_{cm}cx_7sx_8 + s\phi_{cm}sx_7 \\ -c\phi_{cm}sx_7cx_8 - s\phi_{cm}cx_7 \\ c\phi_{cm}cx_8 \\ -s\phi_{cm}/(x_4^2 + x_5^2 + x_6^2)^{1/2}cx_8 \\ c\phi_{cm}/(x_4^2 + x_5^2 + x_6^2)^{1/2} \end{bmatrix}$$

$$\text{and } h(x, t) = \begin{bmatrix} h_1(x, t) \\ h_2(x, t) \end{bmatrix} = \begin{bmatrix} -x_1 s \sigma_t + x_2 c \sigma_t \\ -x_1 s \gamma_t c \sigma_t - x_2 s \gamma_t s \sigma_t + x_3 c \gamma_t \end{bmatrix}$$

The objective of CLOS guidance control is to find a control law to drive the tracking output z to zero. Eq. (5) can be rewritten as

$$\begin{bmatrix} \ddot{z}_1 \\ \ddot{z}_2 \end{bmatrix} = \begin{bmatrix} F_1(x, t) \\ F_2(x, t) \end{bmatrix} + \begin{bmatrix} G_{11}(x, t) & G_{12}(x, t) \\ G_{21}(x, t) & G_{22}(x, t) \end{bmatrix} u(t)$$

$$\ddot{z} \triangleq F(x, t) + G(x, t) \cdot u(t) \quad (5)$$

where $F_1(x, t) = X_0^2 \cdot h_1$, $F_2(x, t) = X_0^2 \cdot h_2$

$$G_{11}(x,t) = X_1 \cdot X_0 \cdot h_1, \quad G_{12}(x,t) = X_2 \cdot X_0 \cdot h_1,$$

$$G_{21}(x,t) = X_1 \cdot X_0 \cdot h_2 \text{ and } G_{22}(x,t) = X_2 \cdot X_0 \cdot h_2$$

$$X_0 h_1 = -\dot{\sigma}_t x_1 c \sigma_t - \dot{\sigma}_t x_2 s \sigma_t - x_4 s \sigma_t + x_5 c \sigma_t$$

$$= -\dot{\sigma}_t R_p c \gamma_t + \dot{\sigma}_t z_2 s \gamma_t - x_4 s \sigma_t + x_5 c \sigma_t$$

$$X_1 X_0 h_1 = -s \phi_{cm} s x_8 s (x_7 - \sigma_t) + c \phi_{cm} c (x_7 - \sigma_t)$$

$$X_2 X_0 h_1 = -c \phi_{cm} s x_8 s(x_7 - \sigma_t) - s \phi_{cm} c(x_7 - \sigma_t)$$

$$\begin{aligned}
 X_1 X_0 h_2 &= (c\gamma_t c x_8 + s\gamma_t s x_8 (x_7 - \sigma_t)) s\phi_{cm} + c\phi_{cm} s\gamma_t s(x_7 - \sigma_t) \\
 X_2 X_0 h_2 &= (c\gamma_t c x_8 + s\gamma_t s x_8 (x_7 - \sigma_t)) c\phi_{cm} - s\phi_{cm} s\gamma_t s(x_7 - \sigma_t) \\
 X_0 h_2 &= (\dot{\sigma}_t s\sigma_t s\gamma_t - \dot{\gamma}_t c\gamma_t s\sigma_t) x_1 - (\gamma_t c\gamma_t s\sigma_t + \dot{\sigma}_t c\sigma_t s\gamma_t) x_2 \\
 &\quad - \dot{\gamma}_t x_3 s\gamma_t - x_4 c\sigma_t s\gamma_t - x_5 s\sigma_t s\gamma_t + x_6 c\gamma_t \\
 &= -\dot{\sigma}_t z_1 s\gamma_t - \dot{\gamma}_t R_p - x_4 c\sigma_t s\gamma_t - x_5 s\sigma_t s\gamma_t + x_6 c\gamma_t \\
 X_0^2 h_1 &= (2\dot{\sigma}_t \dot{\gamma}_t s\gamma_t - \ddot{\sigma}_t c\gamma_t) R_p + \dot{\sigma}_t^2 z_1 + (2\dot{\sigma}_t \dot{\gamma}_t c\gamma_t + \ddot{\sigma}_t s\gamma_t) z_2 \\
 &\quad - 2\dot{\sigma}_t \dot{R}_p c\gamma_t + 2\dot{\sigma}_t \dot{z}_2 s\gamma_t + a_x(t) c x_8 s(x_7 - \sigma_t) \\
 X_0^2 h_2 &= -(\ddot{\gamma}_t + \dot{\sigma}_t^2 s\gamma_t c\gamma_t) R_p - \dot{\sigma}_t z_1 s\gamma_t + (\dot{\sigma}_t^2 s\gamma_t c\gamma_t + \dot{\gamma}_t^2) z_2 \\
 &\quad - 2\dot{\gamma}_t \dot{R}_p - 2\dot{\sigma}_t \dot{z}_1 s\gamma_t + (s x_8 c\gamma_t - c x_8 s\gamma_t c(x_7 - \sigma_t)) \\
 &\quad \cdot a_x(t) - g c\gamma_t \\
 \dot{R}_p &= -(\dot{\sigma}_t s\sigma_t c\gamma_t - \dot{\gamma}_t s\gamma_t c\sigma_t) x_1 - (\dot{\gamma}_t s\gamma_t s\sigma_t - \dot{\sigma}_t c\sigma_t c\gamma_t) x_2 \\
 &\quad + \dot{\gamma}_t x_3 c\gamma_t + x_4 c\gamma_t c\sigma_t + x_5 c\gamma_t s\sigma_t + x_6 s\gamma_t \\
 &= x_4 c\gamma_t c\sigma_t + x_5 c\gamma_t s\sigma_t + x_6 s\gamma_t + \dot{\sigma}_t z_1 c\gamma_t + \dot{\gamma}_t z_2 \quad (7)
 \end{aligned}$$

and

$$\begin{aligned}
 X_0 &= \partial/\partial t + \sum_{i=1}^n f_i(x, t) \cdot \partial/\partial x_i \quad (8) \\
 X_j &= \sum_{i=1}^m g_{j,i}(x) \cdot \partial/\partial x_i \quad j = 1, 2
 \end{aligned}$$

where $f_i(x, t)$, $g_{j,i}(x)$ and x_i are the i^{th} components of $f(x, t)$, $g(x)$ and x respectively.

III. BACKSTEPPING-BASED GUIDANCE LAW DESIGN

Assuming that all parameters of the system (6) are known, the design of Backstepping control for the guidance law is described step-by-step as follows:

Step 1: Define the tracking error

$$e_1(t) = z_d(t) - z(t) \quad (9)$$

where $z_d(t)$ is a desired tracking output. Then the derivative of tracking error can be represented as

$$\dot{e}_1(t) = \dot{z}_d(t) - \dot{z}(t) \quad (10)$$

The $\dot{z}(t)$ can be viewed as a virtual control in above equation.

Define the following stabilizing function

$$\alpha(t) = \dot{z}_d(t) + K_1 e_1(t) \quad (11)$$

where $K_1 = \begin{bmatrix} k_1 & 0 \\ 0 & k_1 \end{bmatrix}$ and k_1 is a positive constant.

The first Lyapunov function is selected as

$$V_1(t) = 0.5 e_1^2(t) \quad (12)$$

Step 2: Define

$$e_2(t) = \alpha(t) - \dot{z}(t) \quad (13)$$

Then the derivative of V_1 with respect to time is

$$\dot{V}_1(t) = e_1(t) \dot{e}_1(t) = -k_1 e_1^2(t) + e_1(t) e_2(t) \quad (14)$$

Step 3: The derivative of $e_2(t)$ is given as

$$\dot{e}_2(t) = \dot{\alpha}(t) - \ddot{z}(t) = \ddot{z}_d(t) + k_1 \dot{e}_1(t) - F(x, t) - G(x, t) u(t) \quad (15)$$

Step 4: If all dynamics system are known, a Backstepping guidance law can be formulated as

$$u^* = G(x, t)^{-1} [\ddot{z}_d(t) + k_1 \dot{e}_1(t) + e_1(t) + K_2 e_2(t) - F(x, t)] \quad (16)$$

where $K_2 = \begin{bmatrix} k_2 & 0 \\ 0 & k_2 \end{bmatrix}$ and k_2 is a positive constant.

Step 5: The second Lyapunov function is defined as

$$V_2(t) = V_1(t) + 0.5 e_2^2(t) \quad (17)$$

Differentiating (17) and using (14) and (15), it is obtained that

$$\begin{aligned}
 \dot{V}_2(t) &= \dot{V}_1(t) + e_2(t) \dot{e}_2(t) \\
 &= -K_1 e_1^2(t) + e_2(t) [e_1(t) + \ddot{z}_d(t) + k_1 \dot{e}_1(t) - F(x, t) - G(x, t) u(t)] \\
 &= -K_1 e_1^2(t) - K_2 e_2^2(t) \leq 0 \quad (18)
 \end{aligned}$$

Since $\dot{V}_2(e_1(t), e_2(t)) \leq 0$, it means that $e_1(t)$ and $e_2(t)$ are bounded. Now define the term:

$$\Omega(t) = K_1 e_1^2(t) + K_2 e_2^2(t) = -\dot{V}_2(e_1(t), e_2(t)) \quad (19)$$

then

$$\int_0^t \Omega(\tau) d\tau = V_2(e_1(0), e_2(0)) - V_2(e_1(t), e_2(t)) \quad (20)$$

Since $V_2(e_1(0), e_2(0))$ is bounded and $V_2(e_1(t), e_2(t))$ is non-increasing and bounded, it can be obtained

$$\lim_{t \rightarrow \infty} \int_0^t \Omega(\tau) d\tau < \infty \quad (21)$$

Also $\dot{\Omega}(t)$ is bounded, so by using Barbalat's Lemma [8], it can be shown that $\lim_{t \rightarrow \infty} \Omega(t) = 0$. This will imply that $e_1(t)$ and $e_2(t)$ converge to zero as $t \rightarrow \infty$. Therefore, the Backstepping Guidance law formulated in (16) is asymptotically stable. The configuration of the proposed Backstepping Guidance Law is shown in Fig. 3.

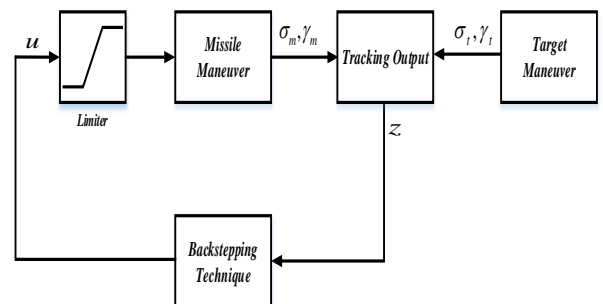


Fig. 3. Backstepping Guidance System.

IV. NUMERICAL SIMULATIONS

In this section, simulations are performed to illustrate the efficiency of the proposed Backstepping guidance law. In order to assess the performance characteristics in a closed-loop engagement scenario, it is important to specify target dynamics. The simplified dynamics of target motion can be given in the inertial frame as follows:

$$\begin{aligned}
 \ddot{x}_t &= -a_{yx} s\psi_t - a_{zx} s\theta_t c\psi_t \\
 \ddot{y}_t &= a_{yx} c\psi_t - a_{zx} s\theta_t s\psi_t \\
 \ddot{z}_t &= a_{zx} c\theta_t - g \\
 \dot{\psi}_t &= a_{yt}/v_t c\theta_t \\
 \dot{\theta}_t &= (a_{zx} - g c\theta_t)/v_t
 \end{aligned} \quad (22)$$

In this paper, three simulation scenarios are examined to justify the effectiveness of the proposed design method. The simulation data and parameter data used for simulation are summarized in Table II.

Table II. Scenario and parameter data used for simulation

States	Scenario 1	Scenario 2	Scenario 3
$x_t(0), y_t(0), z_t(0)$ [m]	2500, 5361.9, 1000	5200, 400, 3000	5200, 5000, 7500
$\dot{x}_t(0), \dot{y}_t(0), \dot{z}_t(0)$ [m/s]	0, -340, 0	-340, 0, 0	0, 0, 500
$\psi_t(0), \theta_t(0)$ [deg]	-90, 0	180, 0	-90, 0
$x_m(0), y_m(0), z_m(0)$ [m]	14.32, 39.34, 3.36	14.56, 5.43, 10.01	28.21, 34.81, 26.52
$\dot{x}_m(0), \dot{y}_m(0), \dot{z}_m(0)$ [m/s]	70.84, 151.92, 28.32	129.65, 12.87, 92.42	250, 250, 400
$\psi_m(0), \theta_m(0)$ [deg]	65, 9.59	20.34, 32.65	45, 54.73
a_x [m/s ²]	$\begin{cases} 340 & 0 \leq t \leq 2 \\ -44.1 & t > 2 \end{cases}$	$\begin{cases} 100 & 0 \leq t \leq 10 \\ -44.1 & t > 10 \end{cases}$	
a_{yt} [m/s ²]	$\begin{cases} 5g & 0 \leq t \leq 2.5 \\ -5g & t > 2.5 \end{cases}$	$\begin{cases} 0g & 0 \leq t \leq 2.5 \\ 0.5g & t > 2.5 \end{cases}$	
a_z [m/s ²]	$\begin{cases} -g & 0 \leq t \leq 2.5 \\ 5g & t > 2.5 \end{cases}$	$\begin{cases} -g & 0 \leq t \leq 2.5 \\ -g & t > 2.5 \end{cases}$	
Guidance command frequency (Hz)	50		
Autopilot damping ratio	0.6		
Autopilot natural frequency (rad/s)	6π		

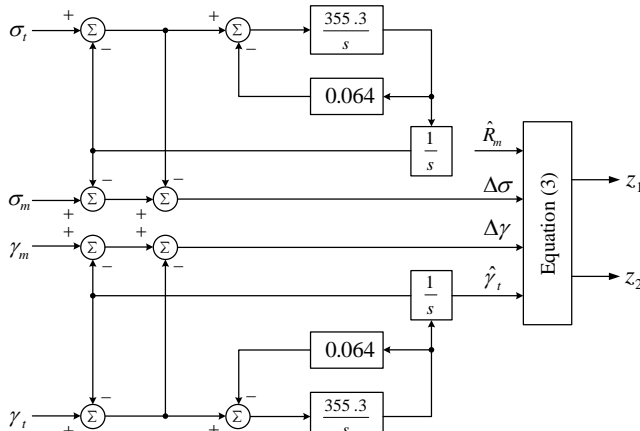


Fig. 4. Block diagram representation of estimation algorithm for guidance information.

The first and second scenarios describes an anti-aircraft scenario. The third one represents an anti-missile scenario. Considered a $30g$ ($g = 9.8m/s^2$) maneuvering limiter to limit the missile's maneuverability. The pitch and yaw autopilot dynamics are selected to be second order linear time-invariant systems and the ground tracker to be a simplified differential tracking system with damping ratio 0.6 and nature frequency 6π rad/s as shown in Fig. 4. The estimated values of $\sigma_t, \gamma_t, \dot{\sigma}_t$ and $\dot{\gamma}_t$, also the measurement data of $\Delta\sigma$ and $\Delta\gamma$, are provided by the ground tracker. To evaluate the influence of measurement noise, random noises with magnitude between ± 0.3 deg are included. m/s^2

The Backstepping guidance law presented in (16) is simulated for the same engagement scenarios. This study adopts the following Backstepping control law:

$$u_{IB}^* = G(x, t)^{-1} [\ddot{z}_d(t) + K_1 \dot{e}_1(t) + e_1(t) + K_2 e_2(t) - F(x, t)]$$

$$K_1 = \begin{bmatrix} 7 & 0 \\ 0 & 7 \end{bmatrix} \text{ and } K_2 = \begin{bmatrix} 20 & 0 \\ 0 & 20 \end{bmatrix}$$

The simulation results for scenarios 1, 2, and 3 are depicted in Figs.5–7, respectively.

Table III. Miss Distance (m)

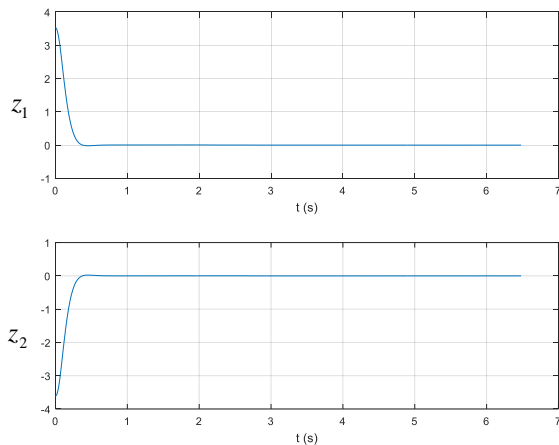
Scenario 1	Scenario 2	Scenario 3
1.8059	2.3319	0.8678

V. CONCLUSION

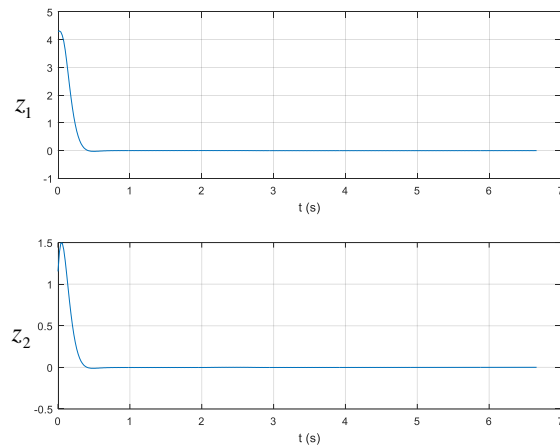
In this paper, a Backstepping control method is applied for the CLOS guidance law design. Simulation results show that the Backstepping guidance law can achieve satisfactory performance and smooth missile trajectories for different engagement scenarios. In addition, from Table III we can notice those small miss distances.

REFERENCES

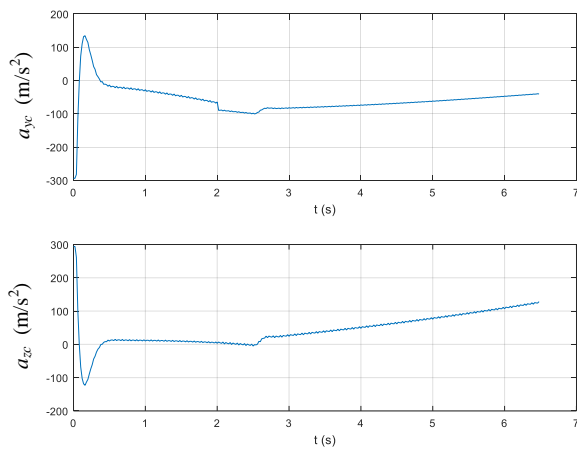
- [1] R. T. Flerning and G. W. Irwin, "Filtering controllers for bank-to-turn CLOS guidance," *Proc. Inst. Elect. Eng. Control Theory Applications*, vol. 134, no. 1, pp. 17–25, 1987.
- [2] I. J. Ha and S. Chong, "Design of a CLOS guidance law via feedback linearization," *IEEE Trans. Aerosp. Electron. Syst.*, vol. 28, no. 1, pp. 51–63, Jan. 1992.
- [3] C. F. Lin, *Modern Navigation, Guidance, and Control Processing*. Englewood Cliffs, NJ: Prentice-Hall, 1991, ch. 6.
- [4] C. D. Yang and C. C. Yang, "A unified approach to proportional navigation," *IEEE Trans. Aerosp. Electron. Syst.*, vol. 33, pp. 557–567, 1997.
- [5] J. Moon, K. Kim, and Y. Kim, "Design of missile guidance law via variable structure control," *J. Guid. Control Dyn.*, vol. 24, no. 4, pp. 659–664, 2001.
- [6] C. M. Lin and Y. F. Peng, "Missile Guidance Law Design Using Adaptive Cerebellar Model Articulation Controller," *IEEE Trans. on Neural Networks*, vol. 16, no. 3, pp. 636–644, May 2005.
- [7] J. J. E. Slotine, and W. Li, *Applied Nonlinear Control*. New Jersey: Prentice-Hall, 1991.



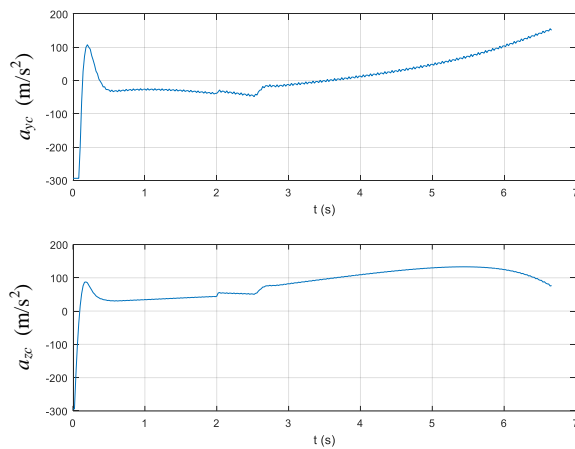
(a) Tracking output (z_1 and z_2)



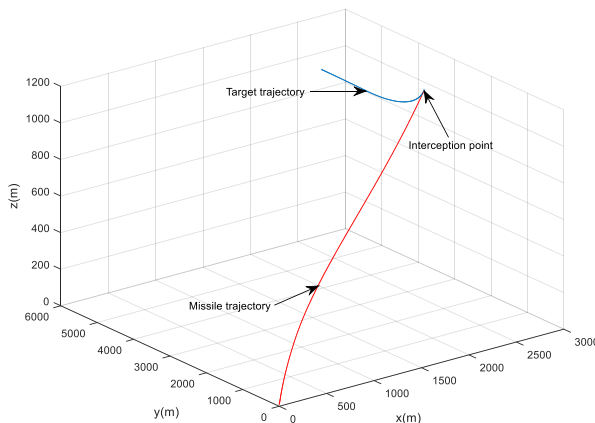
(a) Tracking output (z_1 and z_2)



(b) Acceleration command (a_{yc} and a_{zc})

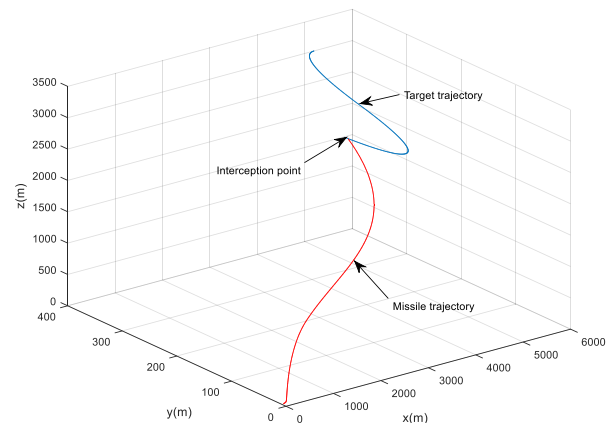


(b) Acceleration command (a_{yc} and a_{zc})



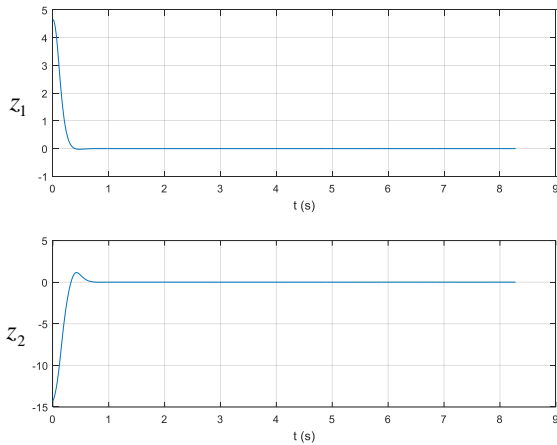
(c) Missile-target trajectory

Fig .5 Engagement scenario 1 with Backstepping guidance law.

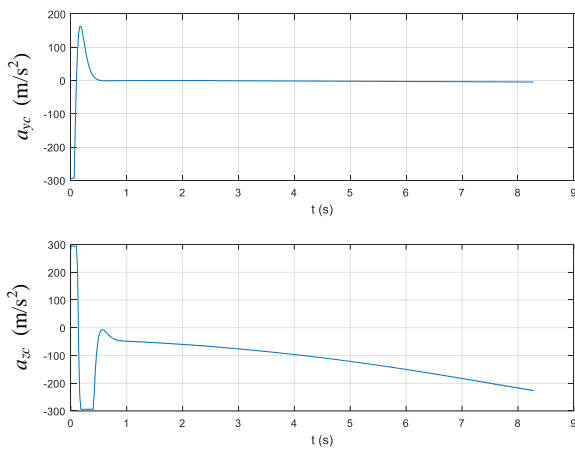


(c) Missile-target trajectory

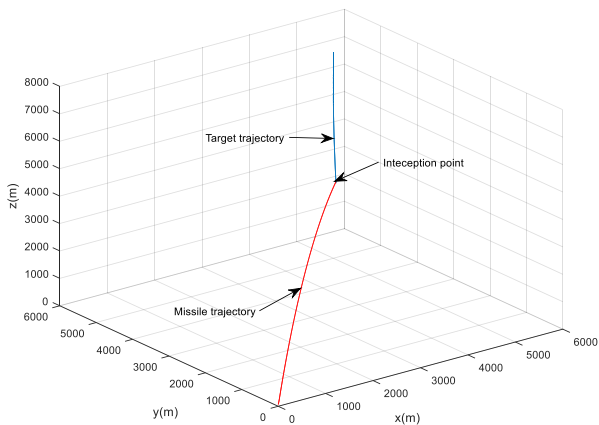
Fig .6 Engagement scenario 2 with Backstepping guidance law.



(a) Tracking output (z_1 and z_2)



(b) Acceleration command (a_{yc} and a_{zc})



(c) Missile-target trajectory

Fig .7 Engagement scenario 3 with Backstepping guidance law.